

Ferromagnetic III–V and II–VI Semiconductors

Tomasz Dietl and Hideo Ohno

Abstract

Recent years have witnessed extensive research aimed at developing functional, tetrahedrally coordinated ferromagnetic semiconductors that could combine the resources of semiconductor quantum structures and ferromagnetic materials systems and thus lay the foundation for semiconductor spintronics. Spin-injection capabilities and tunability of magnetization by light and electric field in Mn-based III–V and II–VI diluted magnetic semiconductors are examples of noteworthy accomplishments. This article reviews the present understanding of carrier-controlled ferromagnetism in these compounds with a focus on mechanisms determining Curie temperatures and accounting for magnetic anisotropy and spin stiffness as a function of carrier density, strain, and confinement. Materials issues encountered in the search for semiconductors with a Curie point above room temperature are addressed, emphasizing the question of solubility limits and self-compensation that can lead to precipitates and point defects. Prospects associated with compounds containing magnetic ions other than Mn are presented.

Keywords: magnetic properties, semiconductor alloys, spin-polarized materials, spintronics, thin films.

Introduction

Early studies of ferromagnetic Cr spinels as well as of rock-salt Eu- and Mn-based chalcogenides led to the observation of a number of outstanding phenomena associated with the interplay between ferromagnetic phenomena and semiconducting properties. However, studies of these ferromagnetic semiconductors were hampered by difficulties in preparation and their relatively low Curie temperatures (T_C), typically below 100 K. Somewhat later, research on diluted magnetic semiconductors (DMSs) was initiated. This family of materials encompasses standard semiconductors, in which a sizable portion of atoms is substituted by elements that produce localized magnetic moments in the semiconductor matrix. Usually, magnetic moments originate from 3d or 4f open shells of transition metals or rare-earth elements (lanthanides), respectively, so that typical examples of DMSs are $\text{Cd}_{1-x}\text{Co}_x\text{Se}$, $\text{Ga}_{1-x}\text{Mn}_x\text{As}$, $\text{Pb}_{1-x}\text{Eu}_x\text{Te}$, and in a sense Si:Er. A strong spin-dependent coupling between the band and localized states accounts for the outstanding properties of DMSs. Ex-

tensive studies of DMSs started in the late 1970s,^{1–3} when appropriately purified Mn was employed to grow bulk II–VI Mn-based alloys by various modifications of the Bridgman method. Compared with the magnetic semiconductors investigated earlier, II–VI DMSs exhibited smaller defect concentrations and were easier to dope with shallow impurities. Accordingly, it was possible to examine a variety of novel spin phenomena by means of powerful magneto-optical and magnetotransport techniques developed to study the standard semiconductors.^{1–4} Disappointingly, however, the dominant interactions between the localized magnetic moments turned out to be antiferromagnetic. This, together with the randomness of magnetic ion distribution, resulted in disordered spin orientations in the absence of an external magnetic field, even at the lowest achievable temperatures.

Recent rapid progress in DMS research that started in the 1990s has stemmed, to a large extent, from the development of crystal growth methods far from thermal

equilibrium, primarily by molecular-beam epitaxy (MBE) but also by laser ablation. These methods have made it possible to obtain DMSs with the content of the magnetic constituent beyond thermal-equilibrium solubility limits. Similarly, doping during the MBE process allows one to substantially increase the electrical activity of shallow impurities. In the case of III–V compounds, in which divalent magnetic atoms supply both spins and holes, the use of low-temperature MBE provides thin films of, for example, $\text{Ga}_{1-x}\text{Mn}_x\text{As}$, with x up to 0.07 and the hole concentration in excess of 10^{20} cm^{-3} .

The discovery of carrier-induced ferromagnetism in zinc-blende III–V compounds containing a few percent Mn^{5,6}—in which T_C can exceed⁷ 100 K—followed by the prediction⁸ and the observation^{9,10} of ferromagnetism in p -type (II, Mn)–VI materials opened up new areas for exploration. We can now consider physical phenomena and device concepts for previously unavailable combinations of quantum structures and magnetism in semiconductors.¹¹ In particular, since in these systems magnetic properties are controlled by the holes in the valence band, the powerful methods developed to change the carrier concentration by electric field and light in semiconductor structures can be employed to alter the magnetic ordering. Such tuning capabilities were demonstrated in (In, Mn)As/(Al, Ga)Sb^{12,13} and (Cd, Mn)Te/(Cd, Zn, Mg)Te:N^{9,14} heterostructures. Notably, the magnetization switching is isothermal, reversible, and fast. Simultaneously, the injection of spin-polarized holes from (Ga, Mn)As to (In, Ga)As quantum wells in p - i - n light-emitting diodes was demonstrated.^{15,16} The injection of spin-polarized electrons, using Zener or Esaki tunneling from p -type (Ga, Mn)As electrodes into n -type GaAs, was also realized.^{17,18} At the same time, outstanding phenomena known from the earlier studies of metallic multilayer structures were observed in ferromagnetic DMSs, including interlayer coupling,^{19,20} exchange-bias behavior,²¹ giant magnetoresistance,¹⁹ and tunneling magnetoresistance.^{22–24} It is an important challenge in materials science to understand ferromagnetism in these compounds. Another challenge is to develop functional semiconductor systems in which Curie temperatures comfortably exceed room temperature and semiconductor and magnetic properties are equally controllable.

This article presents selected materials issues of ferromagnetic III–V and II–VI DMSs. A brief description of models, aimed at a quantitative explanation of the ferromagnetic properties of systems such

as (Ga, Mn)As and (Zn, Cr)Te, is then given, updating previous review papers on the topic.^{25,26}

Transition Metals in II–VI and III–V Semiconductors
Energies of d-Like Levels

A good starting point for the description of DMSs is the Vonsovskii model²⁷ of the electronic structure in materials with localized magnetic moments. According to this model, there are two kinds of relevant electron states: (1) ordinary conduction and valence bands built primarily of outer *s* and *p* orbitals of constituting atoms, and (2) highly localized states derived from open *d* shells of transition metals. The two graphs in Figure 1 depict donor and acceptor *d*-like levels introduced by transition metals to II–VI and III–V compounds, respectively. For either

of these material families, the energies of transition-metal levels are universal, in a sense that they can be presented in one plot if the relative positions of the band edges in particular compounds are shifted according to band offsets known from heterostructure studies.^{28,29} This diagram makes it possible to assess the electrical activity of a given transition-metal impurity in a given host and the variation of its charge state with the extrinsic doping. In particular, transition-metal impurities will introduce electrons if the corresponding donor state is above the bottom of the conduction band (e.g., Sc in CdSe) or holes if the acceptor state is below the top of the valence band (e.g., Mn in GaAs). For a resulting charge state (number of *d*-like electrons), the spin localized on the transition-metal ion assumes the highest possible value, according to Hund’s rule.

Exchange Interactions between Band and d-Like Electrons

The outstanding properties of DMSs stem from the presence of a strong spin-dependent interaction between the electrons in the *sp* bands and those residing on the *d* shells of the transition-metal impurities. This interaction assumes a form of the Heisenberg exchange coupling, $H = -IsS^{2-4,30}$ where *I* describes the strength of the interaction between the carrier spin (*s*) and the transition-metal spin (*S*). In particular, the *s*-type conduction-band electrons experience an exchange potential $I_{sd} \approx 0.2$ eV for the *s*–*d* exchange. The potential exchange is much weaker for the valence-band holes residing mainly on anions. However, there is a symmetry-allowed hybridization of *p* holes and transition-metal *d* states that results in a spin-dependent interaction, the so-called kinetic exchange, characterized by a rather large exchange energy, $|I_{pd}| \approx 1$ eV.^{2-4,30,31} These *sp*–*d* exchange couplings give rise to spin-splitting of bands proportional to the magnetization *M* of the localized magnetic moments.

Substitutional Mn

The thermal-equilibrium solubility of transition-metal impurities is rather low in the materials in question, and low-temperature epitaxy^{5,6} or ion implantation³² have to be employed to introduce a sizable amount of the magnetic constituent. An exception here is the high solubility of Mn in II–VI compounds.^{1,3} This can be attributed to the fact that the Mn *d* states do not significantly perturb *sp*³ bonds because, according to Figure 1, both the lower *d*⁵ (donor) and upper *d*⁶ (acceptor) Hubbard levels are well below and above the band edges, respectively. Thus,

Mn ions neither introduce nor bind carriers, but give rise to the presence of the localized spins ($S = 5/2$). In III–V compounds, in turn, where the transition metals substitute trivalent cations, the Mn acceptor *d* state (*d*⁴) is degenerate with the valence band, at least in the case of antimonides and arsenides. If this is the case, the Mn impurities act as effective mass acceptors, which supply both holes and localized spins, as the Mn ground state corresponds to a *d*⁵ + *h* configuration. Just like in other doped semiconductors, if the Mott criterion is fulfilled, that is, if an average distance between the holes becomes smaller than $2.5a_B$, where *a*_B is the acceptor Bohr radius, the Anderson–Mott insulator-to-metal transition occurs. The fact that the holes cease to be bound to the Mn ions is seen in charge transport,⁷ magnetic circular dichroism,³³ and electron paramagnetic resonance³⁴ measurements on (Ga, Mn)As. Similarly to hole-doped cuprate oxides such as (La, Sr)CuO₄, hybridization between transition-metal *d* shells and anion *p* states may enhance the hole binding energy. The effect is expected to be particularly strong in nitrides and oxides, where a small bond length leads to the strong *p*–*d* interaction.³

Interstitial Mn

Another important materials issue in ferromagnetic DMSs is the existence of an upper limit for the achievable carrier density under thermal-equilibrium conditions. Such a limit can be caused by the finite solubility of a given dopant in a given host. In most cases, however, the effect of self-compensation is involved, which consists of the appearance of compensating point defects once the Fermi level reaches an appropriately high position in the conduction band (donor doping) or low energy in the valence band (acceptor doping). According to particle-induced x-ray emission,³⁶ an increase in the Mn concentration in (Ga, Mn)As not only results in the formation of MnAs precipitates,³⁷ but also in the occupation by Mn of interstitial positions, Mn_i. Since the latter has two unbound 4*s* electrons, it acts as a double donor in GaAs.³⁸ Its formation is triggered by a lowering of the system energy due to removal of the holes from the Fermi level. Moreover, a symmetry analysis demonstrates that the hybridization between the hole *p* bands and Mn_i *d* states is weak and that the exchange interaction between Mn_i and Mn_{Ga} is antiferromagnetic.³⁹ The presence of interstitials appears to explain, therefore, the reentrance of the insulator phase for large Mn concentrations⁷ as well as a substantial increase in magnitudes of both *T*_C (currently

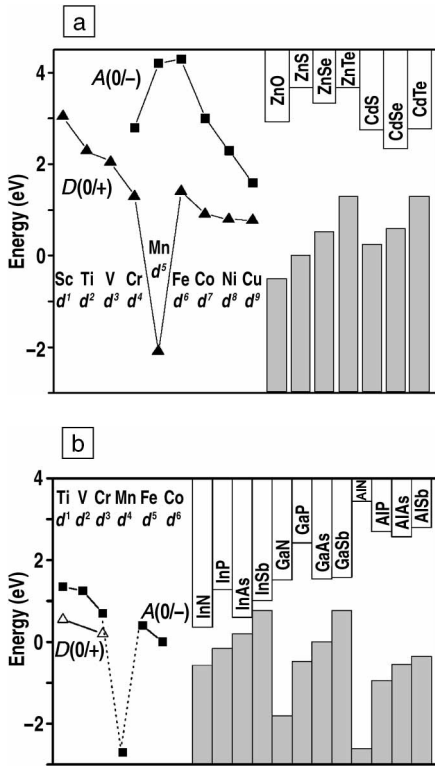


Figure 1. Approximate positions of d-like levels of transition-metal impurities relative to the valence-band edges (shaded bars) and conduction-band edges (white bars) in (a) II–VI and (b) III–V compounds. Triangles represent the *d*^{*N*}/*d*^{*N*−1} donor (D) states (donating the electron, *N* → *N* − 1 becomes positively charged), and squares represent the *d*^{*N*}/*d*^{*N*+1} acceptor (A) states (accepting the electron, *N* → *N* + 1 becomes negatively charged). (Adapted from References 28 and 29.)

up to 160 K) and spontaneous magnetization on annealing^{36,40–43} at temperatures much lower than those affecting other known donor defects in GaAs, such as As antisites As_{Ga} . However, since at high hole concentrations the formation energies and diffusion barriers of all defects tend to decrease, further work is necessary to prove that the interstitials are the only relevant compensators in ferromagnetic DMSs.

Hybrid Structures and Precipitates

There is a large variety of ferromagnetic and ferrimagnetic compounds of transition metals with Group II, III, V, or VI elements that can be grown in the same reactors as the DMSs under discussion. Such compounds are being used as electrodes in spin-injecting and tunneling magnetoresistance devices, in which non-magnetic semiconductors serve as high-quality tunneling barriers.⁴⁴ Furthermore, these magnetic compounds can precipitate during DMS growth or annealing.³⁷ The resulting inclusions, often too small to be detected by standard x-ray diffraction, may contribute to the magnetic properties and sometimes also to the transport and optical properties of the DMS films. Control over the precipitates and elucidation of their influence on material properties are two of the most challenging issues in current DMS studies.

Mechanisms of Interactions between Localized Spins Superexchange

As a result of the aforementioned *sp-d* exchange interaction, the electrons residing in the *sp* bands are either attracted to or repulsed by a given magnetic ion, depending on their spin orientation. This results in a spatial separation of spin-down and spin-up electrons if the bands are entirely occupied, as in insulators or intrinsic semiconductors. Such a separation clearly leads to an antiferromagnetic interaction between neighboring localized spins, a mechanism known as superexchange. Indeed, in the absence of holes, localized spins are antiferromagnetically coupled in Mn-based II–VI^{3,4,30} and III–V^{45,46} DMSs. However, the case of europium chalcogenides (e.g., EuS) and chromium spinels (e.g., $ZnCr_2Se_4$) implies that ferromagnetism is not always related to the presence of free carriers. In fact, a theoretical suggestion has been put forward that superexchange in Cr-based and V-based II–VI compounds can lead to a ferromagnetic order.⁴⁷

Zener/RKKY Models

This reasoning implies the appearance of spin-polarized carrier clouds around each localized spin in *extrinsic* DMSs. Since

the spins of all carriers can assume the same direction if the band is unfilled, a ferromagnetic ordering can emerge, as noted by Zener⁴⁸ in the context of magnetic metals. This ordering can be viewed as driven by lowering of the carriers' energy associated with their redistribution between spin subbands split apart in energy by the exchange interaction. A more detailed quantum treatment indicates, however, that the sign of the interaction between localized spin oscillations with distance, according to the celebrated RKKY (Ruderman–Kittel–Kasuya–Yosida) model.⁴⁹ Nevertheless, as long as the carrier concentration is smaller than that of the localized spins, the RKKY and Zener models lead to the same values of T_C in the mean-field approximation.⁸

Double Exchange

This mechanism operates if the width *V* of the carrier band is smaller than the exchange energy *I*, a situation expected for bands formed from *d* states. As noted in another work by Zener,⁵⁰ spin ordering facilitates carrier hopping over the *d* states, so that the ferromagnetic transition is driven by the lowering of the carrier energy due to an increase in *V*. Accordingly, in such systems spin ordering is always accompanied by a strong increase in the conductivity, an effect leading to so-called colossal magnetoresistance, typically orders of magnitude greater than the giant magnetoresistance occurring in multilayers of magnetic metals. This is the case of manganites such as (La, Sr)MnO₃, where Sr doping introduces holes in the Mn *d* band. So far, there is no evidence for *d*-band transport or for the associated colossal magnetoresistance in III–V and II–VI DMSs.

Mn-Based Ferromagnetic Semiconductors Zener Model of Carrier-Mediated Ferromagnetism

In the mean-field Zener model,⁵¹ the spin magnetization as a function of temperature and magnetic field is determined by minimizing the free energy, consisting of a magnetization term and an electronic term. This is a rather versatile approach, as carrier correlation, confinement, spin-orbit couplings, and quantizing magnetic fields, as well as weak disorder and antiferromagnetic interactions, can be introduced in a controlled way, allowing a quantitative comparison of experimental and theoretical results.^{10,51,52} This formalism directly provides the magnitude of spontaneous magnetization and thus T_C . Furthermore, it makes it possible to determine other important characteristics of

ferromagnetic materials.⁵³ These include magnetic anisotropy,⁵² which determines the crystallographic orientation of the easy axis, and magnetic stiffness,⁵⁴ which describes the robustness of the subsystem against local spin twisting. In the case of strained epitaxial films, the magnitude of magnetic anisotropy is given by the energy difference K_u between the longitudinal and perpendicular orientations of magnetization with respect to the film plane. The magnetic stiffness *A* describes, in turn, the energy penalty associated with the local twisting of the spins from the global direction of magnetization. The determined parameters K_u and *A* for (Ga, Mn)As allows one to assess the domain structure⁵⁵ and magnon dispersion,⁵⁴ that is, to determine how vibration frequencies of spins around the equilibrium orientation depend on the spatial profile of distorted magnetization.

We discuss next some selected properties of ferromagnetic DMSs and compare them with the results of this Zener/RKKY model.

Curie Temperatures

According to Figure 2, theoretical calculations,^{9,10,52} carried out with no adjustable parameters, satisfactorily explain the magnitude of T_C in both (Ga, Mn)As and *p*-type (Zn, Mn)Te. As shown, RKKY cor-

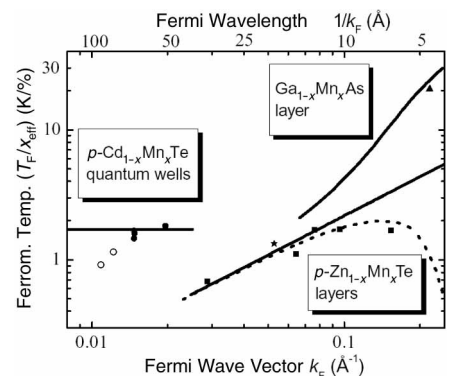


Figure 2. Experimental results (symbols) and calculated values (curves) for the normalized ferromagnetic temperature, $T_F/10^2 \times x_{eff}$, where x_{eff} is the Mn content (excluding the antiferromagnetically coupled nearest-neighbor Mn pairs) versus the wave vector at the Fermi level for $Ga_{1-x}Mn_xAs$ (solid triangle),⁷ $Zn_{1-x}Mn_xTe:N$ (solid squares),¹⁰ quantum wells of $p-Cd_{1-x}Mn_xTe$ (circles),^{9,56} and $Zn_{1-x}Mn_xTe:N:P$ (solid star).⁵⁷ Solid curves are the multiband Zener models⁵² for the three-dimensional and two-dimensional cases; dotted curves include the RKKY (Ruderman–Kittel–Kasuya–Yosida) oscillations.¹⁰ (Adapted from Reference 56.)

rections to the Zener model have to be taken into account in the case of (Zn, Mn)Te. This difference between (Ga, Mn)As and p -(Zn, Mn)Te is associated with the fact that electrically charged Mn pairs are ferromagnetically aligned by the holes in (Ga, Mn)As, while spins of electrically neutral nearest-neighbor Mn pairs remain in antiparallel configurations in (Zn, Mn)Te. Within the Zener model, T_C is proportional to both Mn ion concentration and the density of states for spin excitations. The latter increases with the hole concentration in three-dimensional (3D) systems, but stays constant in 2D systems. Hence, in the 2D case, T_C is expected to not vary with the carrier density and to be enhanced over the 3D value at low carrier densities. Experimental results for modulation-doped p -type (Cd, Mn)Te quantum wells, presented in Figure 2, confirm these expectations, although a careful analysis indicates that disorder-induced band tailing lowers T_C when the Fermi energy approaches the band edge.¹⁴ In 1D systems, in turn, one anticipates a formation of spin-density waves with a wavelength two times shorter than the de Broglie wavelength of the electrons at the Fermi level, a prediction awaiting an experimental confirmation. Owing to the relatively small magnitude of the s - d exchange coupling and density of states, carrier-induced ferromagnetism is expected⁴ and indeed observed only under rather restricted conditions in n -type Mn-based DMSs.^{57,58}

A good agreement between the experimental and theoretical values of T_C in (Ga, Mn)As, p -(Cd, Mn)Te, and p -(Zn, Mn)Te has triggered the extension of the calculations to other Mn-based III–V, II–VI, and IV systems.^{51,52,59} The high-temperature ferromagnetism predicted for nitrides, oxides, and diamond has stimulated a considerable effort aimed at mastering the fabrication of these systems, as has been reviewed recently^{32,35} (see also the article by Chambers and Farrow in this issue). A consensus seems to emerge that (Ga, Mn)N can exhibit ferromagnetic properties persisting above room temperature and involving up to 20% of the Mn spins. Whether this magnetic response comes from Mn substituting for Ga in GaN or from precipitates of another compound is under active debate. In particular, a suggestion has been put forward³⁵ that the strong carrier-induced ferromagnetic coupling, together with the enhanced atom diffusion by the high doping level, may drive a phase separation into ferromagnetic p -type and paramagnetic n -type regions.

Incidentally, the newly developed ferromagnets (Ge, Mn)⁶⁰ and (In, Mn)Sb⁶¹ show

the expected^{52,59} trend in the magnitudes of T_C .

Properties of the Ferromagnetic Phase

In view of spintronic applications, a crucial parameter that characterizes ferromagnetic materials is the degree of spin polarization P of band carriers. Not surprisingly, the magnitude of P increases with the ratio of band splitting for saturated magnetization of localized spins to the Fermi energy. A theoretically expected value of P reaches 80% at low temperatures for typical magnitudes of Mn and hole concentrations in (Ga, Mn)As,⁵² and attains 100% immediately below T_C in modulation-doped (Cd, Mn)Te, where the hole concentration is relatively small.^{9,14}

According to the standard mean-field theory, the growth of the ratio of spontaneous to saturation magnetization M/M_{sat} when the temperature decreases is described by the Brillouin function, which leads to $M/M_{\text{sat}} \sim (T_C - T)^{1/2}$ at T close to T_C and to $1 - M/M_{\text{sat}} \sim T^{5/2}$ in the opposite limit $T \ll T_C$. This would be the case for both M and P in DMSs if P were much smaller than 1. As mentioned earlier, this does not usually occur because no additional carriers are available to further enlarge M at low temperatures. As a result, the relation between M and P ceases to be linear, and neither of them follows the Brillouin function form on cooling below T_C ,⁵² even if other effects, such as a decrease in M by magnons (spin wave excitations), disorder, and T_C gradient in the film, are unimportant.

It is well known that the orbital momentum of the majority hole subbands depends on strain and confinement. Hence, magnetic anisotropy (easy-axis direction), which exists due to the spin-orbit interaction in the valence band, can be manipulated by adjusting the lattice parameter of the substrate. This is because the growth of the DMS films in question is usually pseudomorphic despite lattice mismatch, that is, no misfit dislocations are formed, but the in-plane lattice parameter of the film assumes the substrate value. Theoretical results show that the orientation of the easy axis with respect to the film plane depends on whether the epitaxial strain is compressive or tensile, in agreement with the early experimental studies of (In, Mn)As⁶² and (Ga, Mn)As.⁶³ However, magnetic anisotropy at a given strain is predicted to vary with the degree of the occupation of particular hole subbands.⁵² This, in turn, is determined by the ratio of the valence-band exchange splitting to the Fermi energy and thus by the magnitude of spontaneous magnetization, which

depends on temperature. As shown in Figure 3, such a temperature-induced switching of the easy-axis direction has recently been detected in samples with appropriately low hole densities.^{64,65}

Finally, we note that a large magnitude of spin stiffness in (Ga, Mn)As,⁵⁴ which can be traced back to the multiband character and p symmetry of the valence-band states, results in large energies of both domain walls and spin wave excitations. This accounts for excellent micromagnetic properties of this system^{55,66,67} and *a posteriori* explains the quantitative accuracy of the mean-field approximation. Similarly, it becomes possible to describe quantitatively the magnitude of the anomalous Hall effect and anisotropic magnetoresistance in this material.⁶⁸

Beyond Mn-Based Compounds Ferromagnetism in Cr-Based II–VI DMSs

As already noted, ferromagnetic superexchange was predicted for Cr-based II–VI DMSs.⁴⁷ A ferromagnetic ground state in these systems is also expected from more recent *ab initio* computations⁶⁹ that suggest, however, that double exchange rather than superexchange is involved.

Recent work⁷⁰ on (Zn, Cr)Te has led to the observation of ferromagnetism by both direct magnetization measurements and magnetic circular dichroism (MCD). According to the MCD results presented in Figure 4, ferromagnetism persists up to room temperature in a sample containing 20% of Zn replaced by Cr. Since no electrical conductance is detected, the ferromagnetic double exchange does not appear to operate. At the same time, for the currently accepted values of the parameters, the observed magnitude of T_C is too high to be explained within the superexchange scenario, but by adjusting parameters within the physically acceptable range, such a scenario becomes plausible. Indications of ferromagnetism below 100 K have also been found in (Zn, Cr)Se.⁷¹ The enhanced magnetic response has been assigned to precipitates, as the apparent T_C does not scale with the Cr concentration and is close to the T_C of the spinel semiconductor ZnCr₂Se₄. Nonetheless, independent of the microscopic nature of ferromagnetic ordering, the large magnitude of the MCD of Figure 4 suggests possible applications of this system in photonic devices such as Faraday optical insulators.

Other Systems

With no doubt, independent control of electronic and magnetic properties and, in particular, the availability of n -type tetra-

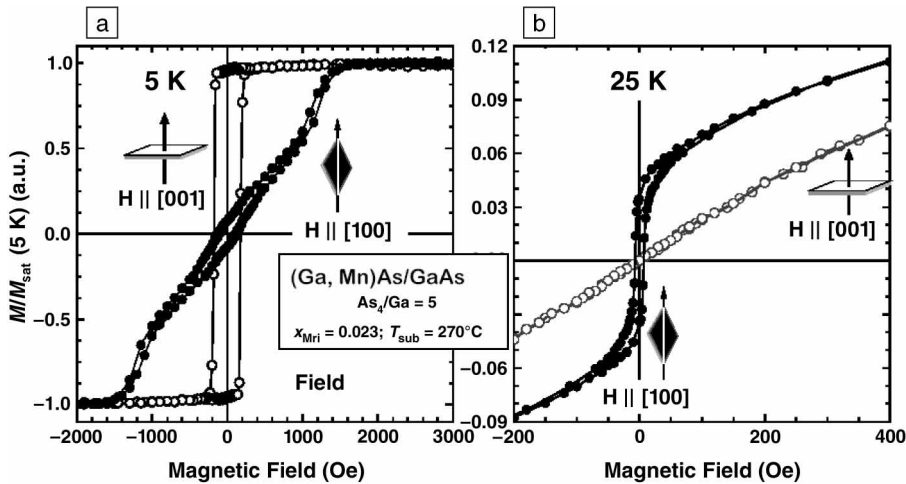


Figure 3. Magnetization loops at (a) 5 K and (b) 25 K for parallel (solid symbols) and perpendicular (open symbols) orientations of the (Ga, Mn)As/GaAs(001) epilayer with respect to the external magnetic field. The reversed character of the hysteresis loops indicates the flip of the easy-axis direction between these two temperatures. The Mn content and the growth temperatures are denoted by x_{Mn} and T_{sub} , respectively. Magnetization is normalized by its saturation value M_{sat} . (After Reference 66.)

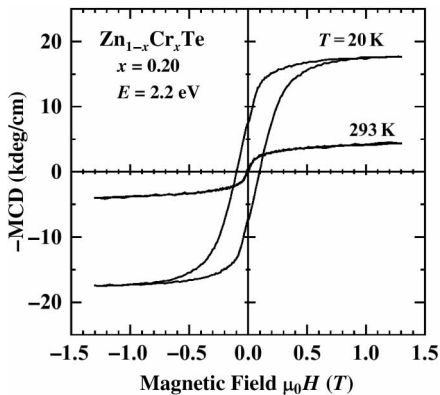


Figure 4. Magnetic-field dependence of magnetic circular dichroism (MCD) in a $Zn_{1-x}Cr_xTe$ ($x = 0.20$) film at photon energy $E = 2.2$ eV and temperatures of 20 K and 293 K, indicating the presence of ferromagnetic ordering persisting up to room temperature. The minus sign shows that the MCD signal at $E = 2.2$ eV is negative and the unit is in rotation angle of polarization vector per centimeter. (After Reference 71.)

hedrally coordinated ferromagnetic compounds would considerably enlarge the impact of semiconductor spintronics. Unfortunately, in the case of the (Zn, Cr)–VI DMSs discussed earlier, according to the level diagram presented in Figure 1, carriers introduced by shallow impurities will be trapped by the d states. However, for a sufficiently high density of the trapped

carriers, the Mott criterion will be fulfilled, so that the double exchange interaction and charge transport through d band will appear in such systems. Desired material properties, such as divergent magnetic susceptibility and spontaneous magnetization, can be produced by a strong antiferromagnetic superexchange interaction. The idea here is to synthesize a ferrimagnetic system that would consist of antiferromagnetically coupled alternating layers containing different magnetic cations, for example, Mn and Co in a II–VI matrix.⁴ Finally, since in general III–V compounds can be doped more easily with impurities that are electrically active, whereas II–VI materials support a greater concentration of transition metals, the suggestion has been put forward to grow magnetic III–V/II–VI short-period superlattices⁷² in which a charge transfer to the magnetic layers will increase T_C .

Conclusions

Recent years have witnessed remarkable progress in the development of new materials systems that show novel capabilities such as the manipulation of ferromagnetism by electric field and light. Thus, these materials can already be used to develop quantum information devices. On the other hand, further work is needed to demonstrate functional ferromagnetic compounds for room-temperature semiconductor spintronics. This will require researchers to overcome the limitations imposed by solubility limits and self-

compensation. On the theoretical side, carrier-controlled ferromagnetic semiconductors combine the intricate properties of charge-transfer insulators and strongly correlated disordered metals with the physics of defect and band states in heavily doped semiconductors. Accordingly, despite important advances in the theoretical understanding of these systems, their description from first principles may take some time.

Acknowledgments

This work has been supported by the Exploratory Research for Advanced Technology (ERATO) project, “Semiconductor Spintronics,” of the Japan Science and Technology Corporation. The work by T. Dietl in Poland is partly supported by the State Committee for Scientific Research as well as by FENIKS (Ferromagnetic Semiconductors and Novel Magnetic Semiconductor Heterostructures for Improved Knowledge on Spintronics) and AMORE (Advanced Magnetic Oxides for Responsive Engineering), both projects of the European Commission. The work by T. Dietl in Germany at Regensburg University is supported by the Alexander von Humboldt Foundation. The work by H. Ohno is partly supported by the Information Technologies Program of Research Revolution 2002 (RR2002) of MEXT (the Japanese Ministry of Education, Culture, Sports, Science, and Technology) and by a grant-in-aid from the Japan Society for the Promotion of Science.

References

1. R.R. Gałazka, in *Proc. 14th Int. Conf. on Physics of Semiconductors*, Inst. Phys. Conf. Ser. 43, edited by B.L.H. Wilson (Institute of Physics, Bristol, 1978) p. 133
2. T. Dietl, in *Physics in High Magnetic Fields*, Springer Series in Solid-State Physics, Vol. 24, edited by S. Chikazumi and N. Miura (Springer, Berlin, 1981) p. 344.
3. J.K. Furdyna and J. Kossut, eds., *Diluted Magnetic Semiconductors, Semiconductors and Semimetals*, Vol. 25, R.K. Willardson and A.C. Beer, series editors (Academic Press, New York, 1988).
4. T. Dietl, in *Materials, Properties and Preparations*, edited by S. Mahajan, *Handbook on Semiconductors*, 2nd ed., Vol. 3B, edited by T.C. Moss (North-Holland, Amsterdam, 1994) p. 1251.
5. H. Ohno, H. Munekata, T. Penney, S. von Molnár, and L.L. Chang, *Phys. Rev. Lett.* **68** (1992) p. 2664.
6. H. Ohno, A. Shen, F. Matsukura, A. Oiwa, A. Endo, S. Katsumoto, and Y. Iye, *Appl. Phys. Lett.* **69** (1996) p. 363.
7. F. Matsukura, H. Ohno, A. Shen, and Y. Sugawara, *Phys. Rev. B* **57** (1998) p. R2037.
8. T. Dietl, A. Haury, and Y. Merle d’Aubigné, *Phys. Rev. B* **55** (1997) p. R3347.
9. A. Haury, A. Wasiela, A. Arnoult, J. Cibert, S. Tatarenko, T. Dietl, and Y. Merle d’Aubigné, *Phys. Rev. Lett.* **79** (1997) p. 511.
10. D. Ferrand, J. Cibert, A. Wasiela, C.

- Bourgognon, S. Tatarenko, G. Fishman, T. Andrearczyk, J. Jaroszyński, S. Koleśnik, T. Dietl, B. Barbara, and D. Dufeu, *Phys. Rev. B* **63** 085201 (2001).
11. H. Ohno, *Science* **281** (1998) p. 951.
12. S. Koshihara, A. Oiwa, M. Hirasawa, S. Katsumoto, Y. Iye, C. Urano, H. Takagi, and H. Munekata, *Phys. Rev. Lett.* **78** (1997) p. 617.
13. H. Ohno, D. Chiba, F. Matsukura, T. Omiya, E. Abe, T. Dietl, Y. Ohno, and K. Ohtani, *Nature* **408** (2000) p. 944.
14. H. Boukari, P. Kossacki, M. Bertolini, D. Ferrand, J. Cibert, S. Tatarenko, A. Wasiela, J.A. Gaj, and T. Dietl, *Phys. Rev. Lett.* **88** 207204 (2002).
15. Y. Ohno, D.K. Young, B. Beschoten, F. Matsukura, H. Ohno, and D.D. Awschalom, *Nature* **402** (1999) p. 790.
16. D.K. Young, E. Johnston-Halperin, D.D. Awschalom, Y. Ohno, and H. Ohno, *Appl. Phys. Lett.* **80** (2002) p. 1598.
17. M. Kohda, Y. Ohno, K. Takamura, F. Matsukura, and H. Ohno, *Jpn. J. Appl. Phys. Part 2: Lett.* **40** (2001) p. L1274.
18. E. Johnston-Halperin, D. Lofgreen, R.K. Kawakami, D.K. Young, L. Coldren, A.C. Gossard, and D.D. Awschalom, *Phys. Rev. B* **65** 041306(R) (2002).
19. D. Chiba, N. Akiba, F. Matsukura, Y. Ohno, and H. Ohno, *Appl. Phys. Lett.* **77** (2000) p. 1873.
20. J. Sadowski, R. Mathieu, P. Svedlindh, M. Karlsteen, J. Kanski, Y. Fu, J.T. Domagała, W. Szuskiewicz, B. Hennion, D.K. Maude, R. Airey, and G. Hill, *Thin Solid Films* **412** (2002) p. 122.
21. X. Liu, Y. Sasaki, and J.K. Furdyna, *Appl. Phys. Lett.* **79** (2001) p. 2414.
22. M. Tanaka and Y. Higo, *Phys. Rev. Lett.* **87** 026602 (2001).
23. R. Mattana, J.-M. George, H. Jaffrès, F. Nguyen Van Dau, A. Fert, B. Lépine, A. Guivarčh, and G. Jézéquel, *Phys. Rev. Lett.* **90** 166601 (2003).
24. D. Chiba, F. Matsukura, and H. Ohno, 8th Symposium on the Physics and Application of Spin Related Phenomena in Semiconductors, Extended Abstracts (2002) p. 250.
25. T. Dietl, *Semicond. Sci. Technol.* **17** (2002) p. 377.
26. F. Matsukura, H. Ohno, and T. Dietl, in *Handbook of Magnetic Materials*, Vol. 14, edited by K.H.J. Buschow (Elsevier, Amsterdam, 2002) p. 1.
27. S.V. Vonsovskii, *Magnetism* (John Wiley & Sons, New York, 1974).
28. A. Zunger, in *Solid State Physics*, Vol. 39, edited by H. Ehrenreich and D. Turnbull (Academic Press, New York, 1986) p. 275.
29. J.M. Langer, C. Delerue, M. Lannoo, and H. Heinrich, *Phys. Rev. B* **38** (1988) p. 7723.
30. P. Kacman, *Semicond. Sci. Technol.* **16** (2001) p. R25.
31. In the literature on diluted magnetic semiconductors (see References 1–4), the $sp-d$ exchange integrals are usually denoted by α and β according to $\alpha = I_{sd}/N_0$ and $\beta = I_{pd}/N_0$, where N_0 is the total cation concentration.
32. S.J. Pearton, C.R. Abernathy, M.E. Overberg, G.T. Thaler, D.P. Norton, N. Theodoropoulou, A.F. Hebard, Y.D. Park, F. Ren, J. Kim, and L.A. Boatner, *J. Appl. Phys.* **93** (2003) p. 1.
33. J. Szczytko, W. Bardyszewski, and A. Twardowski, *Phys. Rev. B* **64** 075306 (2001).
34. O.M. Fedorych, E.M. Hankiewicz, Z. Wilamowski, and J. Sadowski, *Phys. Rev. B* **66** 045201 (2002).
35. T. Dietl, in *Proc. 5th Int. Conf. on Nitride Semiconductors*, Nara, Japan, 2003, *Phys. Status Solidi B*, in press (e-print: <http://arxiv.org/abs/cond-mat/030511>).
36. K.M. Yu, W. Walukiewicz, T. Wojtowicz, I. Kuryliszyn, X. Liu, Y. Sasaki, and J.K. Furdyna, *Phys. Rev. B* **65** 201303(R) (2002).
37. J. De Boeck, R. Oesterholt, A. Van Esch, H. Bender, C. Bruynseraede, C. Van Hoof, and G. Borghs, *Appl. Phys. Lett.* **68** (1996) p. 2744.
38. F. Mácá and J. Mašek, *Phys. Rev. B* **65** 235209 (2002).
39. J. Blinowski and P. Kacman, *Phys. Rev. B* **67** 121204(R) (2003).
40. T. Hayashi, Y. Hashimoto, S. Katsumoto, and Y. Iye, *Appl. Phys. Lett.* **78** (2001) p. 1691.
41. K.C. Ku, S.J. Potashnik, R.F. Wang, S.H. Chun, P. Schiffer, N. Samarth, M.J. Seong, A. Mascarenhas, E. Johnston-Halperin, R.C. Meyers, A.C. Gossard, and D.D. Awschalom, *Appl. Phys. Lett.* **82** (2003) p. 2302.
42. K.W. Edmonds, K.Y. Wang, R.P. Campion, A.C. Neuman, C.T. Foxon, B.L. Gallagher, and P.C. Main, *Appl. Phys. Lett.* **81** (2002) p. 3010; K.W. Edmonds, K.Y. Wang, R.P. Campion, A.C. Neuman, N.R.S. Farley, B.L. Gallagher, and C.T. Foxon, *Appl. Phys. Lett.* **81** (2002) p. 4991.
43. D. Chiba, K. Takamura, F. Matsukura, and H. Ohno, *Appl. Phys. Lett.* **82** (2003) p. 3020.
44. M. Tanaka, *Semicond. Sci. Technol.* **17** (2002) p. 327.
45. S. von Molnár, H. Munekata, H. Ohno, and L.L. Chang, *J. Magn. Magn. Mater.* **93** (1991) p. 356.
46. Y. Satoh, D. Okazawa, A. Nagashima, and J. Yoshino, *Physica E* **10** (2001) p. 196.
47. J. Blinowski, P. Kacman, and J.A. Majewski, *Phys. Rev. B* **53** (1996) p. 9524; *J. Cryst. Growth* **159** (1996) p. 972.
48. C. Zener, *Phys. Rev.* **81** (1951) p. 440; *Phys. Rev.* **83** (1951) p. 299.
49. K. Yosida, *Theory of Magnetism* (Springer, Berlin, 1996).
50. C. Zener, *Phys. Rev.* **82** (1951) p. 403.
51. T. Dietl, H. Ohno, F. Matsukura, J. Cibert, and D. Ferrand, *Science* **287** (2000) p. 1019.
52. T. Dietl, H. Ohno, and F. Matsukura, *Phys. Rev. B* **63** 195205 (2001).
53. R. Skomski and C.M. Coey, *Permanent Magnetism* (Institute of Physics, Bristol, 1999).
54. J. König, T. Jungwirth, and A.H. MacDonald, *Phys. Rev. B* **64** 184423 (2001).
55. T. Dietl, J. König, and A.H. MacDonald, *Phys. Rev. B* **64** 241201(R) (2001).
56. J. Cibert, D. Ferrand, H. Boukari, S. Tatarenko, A. Wasiela, P. Kossacki, and T. Dietl, *Physica E* **13** (2002) p. 489.
57. T. Andrearczyk, J. Jaroszyński, M. Sawicki, L. Van Khoi, T. Dietl, D. Ferrand, C. Bourgognon, J. Cibert, S. Tatarenko, T. Fukumura, Z. Jin, H. Koinuma, and M. Kawasaki, in *Proc. 25th Int. Conf on Physics of Semiconductors*, edited by N. Miura and T. Ando (Springer, Berlin, 2001) p. 235.
58. J. Jaroszyński, T. Andrearczyk, G. Karczewski, J. Wróbel, T. Wojtowicz, E. Papis, E. Kamińska, A. Piotrowska, D. Popović, and T. Dietl, *Phys. Rev. Lett.* **89** 266802 (2002).
59. T. Jungwirth, J. König, J. Sinova, J. Kucera, and A.H. MacDonald, *Phys. Rev. B* **66** 012402 (2002).
60. Y.D. Park, A.T. Hanbicki, S.C. Erwin, C.S. Hellberg, J.M. Sullivan, J.E. Mattson, T.F. Ambrose, A. Wilson, G. Spanos, and B.T. Jonker, *Science* **295** (2002) p. 652.
61. T. Wojtowicz, G. Cywiński, W.L. Lim, X. Liu, M. Dobrowolska, J.K. Furdyna, K.M. Yu, W. Walukiewicz, G.B. Kim, M. Cheon, X. Chen, S.M. Wang, and H. Luo, *Appl. Phys. Lett.* **82** (2003) p. 4310.
62. H. Munekata, A. Zaslavsky, P. Fumagalli, and R.J. Gambino, *Appl. Phys. Lett.* **63** (1993) p. 2929.
63. A. Shen, H. Ohno, F. Matsukura, Y. Sugawara, N. Akiba, T. Kuroiwa, A. Oiwa, A. Endo, S. Katsumoto, and Y. Iye, *J. Cryst. Growth* **175/176** (1997) p. 1069.
64. K. Takamura, F. Matsukura, D. Chiba, and H. Ohno, *Appl. Phys. Lett.* **81** (2002) p. 2590.
65. M. Sawicki, F. Matsukura, A. Idziaszek, G.M. Schott, G. Karczewski, C. Ruester, G. Schmidt, L.W. Molenkamp, and T. Dietl, *J. Supercond./Novel Magn.* **16** (2003) p. 3 (e-print: <http://arxiv.org/abs/cond-mat/0212511>).
66. T. Shono, T. Hasegawa, T. Fukumura, F. Matsukura, and H. Ohno, *Appl. Phys. Lett.* **77** (2000) p. 1363.
67. U. Welp, V.K. Vlasko-Vlasov, X. Liu, J.K. Furdyna, and T. Wojtowicz, *Phys. Rev. Lett.* **90** 167206 (2003).
68. T. Jungwirth, J. Sinova, K.Y. Wang, K.W. Edmonds, R.P. Campion, B.L. Gallagher, C.T. Foxon, Q. Nu, and A.H. MacDonald, *Appl. Phys. Lett.* **83** (2003) p. 320.
69. K. Sato and H. Katayama-Yoshida, *Semicond. Sci. Technol.* **17** (2002) p. 367.
70. H. Saito, V. Zayets, S. Yamagata, and K. Ando, *Phys. Rev. Lett.* **90** 207202 (2003).
71. G. Karczewski, M. Sawicki, V. Ivanov, C. Ruester, G. Grabecki, F. Matsukura, L.W. Molenkamp, and T. Dietl, *J. Supercond./Novel Magn.* **16** (2003) p. 55.
72. T. Kamatani and H. Akai, *Physica E* **10** (2001) p. 157. □

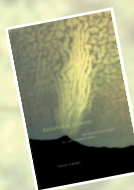
MRS 2003 FALL MEETING SPECIAL EVENT

Felice Frankel

Symposium X Speaker • Wednesday, December 3 • 12:45 pm

Grand Ballroom • Sheraton Hotel

“Envisioning Materials Research—Finding A New Visual Voice”



After Symposium X, meet the speaker!

Envisioning Science
Book Signing

Wednesday, December 3 • 2:30 pm – 4:00 pm
Publications Sales • Level 2, Hynes